Pressure-dependent thermal conductivity in Al, W, and Pt: Role of electrons and phonons

Xinyu Zhang,[1] Shouhang Li,[2] Ao Wang,[1] and Hua Bao[1,*]
[1]*University of Michigan–Shanghai Jiao Tong University Joint Institute, Shanghai Jiao Tong University, Shanghai 200240, People's Republic of China*
[2]*College of Mechanical Engineering, Donghua University, Shanghai 201620, People's Republic of China*

(Received 7 April 2022; revised 24 July 2022; accepted 23 August 2022; published 26 September 2022)

Understanding the pressure dependence on thermal transport of metals is crucial for high-pressure applications and fundamental research in earth science. As high-pressure thermal measurements are challenging, the theoretical approach and first-principles methods are widely adopted to investigate the pressure-dependent thermal transport in metals. However, these approaches are generally limited to the free-electron metals and the phonon contributions are neglected. The mechanisms behind the pressure effect on thermal transport of metals are not fully addressed. In this work, we implement rigorous mode-level first-principles calculations to reveal different mechanisms behind the pressure-dependent electronic and phonon thermal conductivity in aluminum (Al), tungsten (W), and platinum (Pt). While the overall thermal conductivity values of the three metals all increase with pressure, the mechanisms are different. For the electronic thermal conductivity part, the main contribution for the positive pressure effect on free-electron metal Al is the decrease of the electron-phonon scattering rate, while the dominant contribution in Pt and W, whose *d* state electrons are abundant around the Fermi energy, is the increase of electron group velocity. Phonon thermal conductivity of Pt and Al is found to increase with pressure, but the rates of increase are different. In contrast, phonon thermal conductivity of W is nearly independent with pressure. Such pressure invariance is due to the competing effect between phonon lifetime decrease and phonon group velocity increase under pressure.

DOI: 10.1103/PhysRevB.106.094313

I. INTRODUCTION

Thermal conductivity under pressure is crucial for many applications, such as the thermal evolution of the Earth's core [1–4], high-pressure synthesis of materials [5–8], and manufacturing apparatuses for high-pressure scenarios [9,10]. The pressure-dependent thermal conductivity for many nonmetallic materials has been investigated [2,11,12], and it has been generally found that the thermal conductivity increases with pressure [13]. The underlying pressure-dependent phonon transport mechanism has been carefully discussed [12,14]. In comparison, the pressure-dependent thermal transport in metals is less explored [15–17]. Different from nonmetallic materials, the thermal transport in metals is contributed by both electrons and phonons. The scattering and transport of these two carriers lead to relatively more complicated pressure-dependent thermal transport in metals [18,19].

High-pressure thermal measurements have been quite challenging and therefore have undergone slow development [20]. There are two main difficulties: The first is to maintain a high-pressure environment and the second is to measure physical properties under high pressure. In recent years, these difficulties were partly solved by methods like the combination of the diamond anvil cell [21] and the modern micro- and nanoprobing technology [22]. Although it is now possible to conduct thermal measurements under the pressure of hundreds of GPa [20], it is still not an easy task to perform such experiments. As such, there are quite limited available experimental thermal conductivity data for metals under pressure [23]. In addition, the existing data of high-pressure thermal measurements are scattered, leading to controversy. For example, the measured thermal conductivity of iron at similar temperature and pressure in different experiments ranges from 40 to 226 W/mK [24,25]. Moreover, the experiments can only provide thermal conductivity values, while the underlying mechanisms, especially the separation of electron and phonon contributions to the thermal conductivity, are a long-standing challenge. On the other hand, theoretical models were developed to understand the pressure-dependent thermal conductivity of metals. Since electrons are believed to be the main heat carriers in most metals, an analytical model for the pressure-dependent electronic thermal conductivity was developed by Bohlin [26] based on Bloch-Grüneisen theory [27,28], and subsequently modified by Sundqvist and co-workers [29]. According to this model, the electronic thermal conductivity increases with pressure due to the reduced electron-phonon coupling strength. This model is fairly accurate in predicting the electronic thermal conductivity at a relatively low-pressure regime for free-electron metals [29]. However, due to the limitation of the free-electron approximation, this model cannot accurately determine the pressure dependence of thermal conductivity for complex transition metals [29].

Recent advances in first-principles methods allow more quantitative investigations for pressure-dependent thermal conductivity of metals [15–17,30,31]. Allen's model [32],

*hua.bao@sjtu.edu.cn

which is the lowest-order variational approximation of the solution to the Boltzmann transport equation, has been combined with first-principles methods to obtain the electron thermal transport properties of metallic systems. This method has been adopted to study the pressure effect of free-electron metals, including Cu, Al, Au, and Ag [15,33]. Similar to the theoretical model derived by Bohlin [26], their results also predict a positive correlation between electronic thermal conductivity and pressure, due to the decreased electron-phonon interaction under pressure. However, this method still shows non-negligible deviations from experiments for metals with complex electronic structure [34]. More accurate first-principles methods, such as the Korringa-Kohn-Rostoker method combined with the coherent potential approximation [30,31], and the first-principles molecular dynamics [30,31], are used to predict the pressure-dependent thermal conductivity of metals. However, the phonon transport is not considered in these methods. Reviewing the previous studies, although significant progress has been made to predict and understand the pressure dependence of thermal conductivity in metals, there are still two main limitations. First, the contribution of phonons, which has been shown to be important in many metals under ambient pressure [35–37], is often neglected. Second, the current understanding is that, at intermediate temperature, the pressure dependence of electronic thermal conductivity is due to the reduced electron-phonon coupling. Although this is valid for free-electron metals, whether this mechanism can be extended to metals with complex electronic structures remains unclear.

In this work, we aim to develop better understanding of the pressure effect on the electronic and phonon thermal conductivity in metals. We adopt the mode-level first-principles calculation method, which is proved to be accurate when applied to different types of metals [38,39] at ambient pressure. Meanwhile, this method naturally includes both the electron and phonon contributions at the mode level, which allows us to examine the detailed mechanisms of the pressure dependence of thermal conductivity. Three representative metals, including, Al, Pt, and W, are chosen as representative prototypes in this work. Al is a typical free-electron metal, Pt possesses a complex Fermi surface [40], and W is known for its high phonon contribution to its total thermal conductivity [41]. Pressure-dependent electronic and phonon thermal conductivity of these three metals are accurately predicted using the mode-level first-principles method. Moreover, a detailed mode-level analysis is also carried out to understand the mechanisms for the pressure dependence of thermal conductivity.

II. MODE-LEVEL FIRST-PRINCIPLES METHOD

Here we adopt the mode-level first-principles calculation to study pressure-dependent electronic and phonon thermal conductivity in metals. The details of our methodology have been discussed in our previous works [38,39,42]. For brevity, we use the Boltzmann transport equations (BTEs) with relaxation time approximation to calculate the electrical conductivity ($\sigma^{\alpha\beta}$) and electronic thermal conductivity ($\kappa_{el}^{\alpha\beta}$) [42],

$$\sigma^{\alpha\beta} = -\frac{q^2}{N_{\mathbf{k}}V}\sum_{n\mathbf{k}} v_{n\mathbf{k}}^{\alpha} v_{n\mathbf{k}}^{\beta} \tau_{n\mathbf{k}}^{\sigma}(\varepsilon_{n\mathbf{k}}, \zeta, T)\frac{\partial f^0(\varepsilon_{n\mathbf{k}}, \zeta, T)}{\partial \varepsilon_{n\mathbf{k}}}, \quad (1)$$

$$\kappa_{el}^{\alpha\beta} = \frac{1}{N_{\mathbf{k}}V}\sum_{n\mathbf{k}} -\frac{(\varepsilon_{n\mathbf{k}} - \zeta)^2}{T} v_{n\mathbf{k}}^{\alpha} v_{n\mathbf{k}}^{\beta} \tau_{n\mathbf{k}}^{\kappa}(\varepsilon_{n\mathbf{k}}, \zeta, T) \times \frac{\partial f^0(\varepsilon_{n\mathbf{k}}, \zeta, T)}{\partial \varepsilon_{n\mathbf{k}}}, \quad (2)$$

where α and β are the Cartesian coordinate components, q is the electron charge, $N_{\mathbf{k}}$ is the total number of $\mathbf{k}$ points in the first Brillouin zone and V is the volume of the unit cell, $v_{n\boldsymbol{k}}$ is the electron group velocity at mode $n\mathbf{k}$ (n is the band index; $\mathbf{k}$ is the wave vector), ε is the electron energy, f^0 is the equilibrium electron distribution function, ζ is the Fermi energy, and τ^{σ} and τ^{κ} are the momentum and energy relaxation time, respectively [42]. Considering the following expression of electron specific heat,

$$C_{el} = \frac{1}{N_{\mathbf{k}}V}\sum_{n\mathbf{k}} -\frac{(\varepsilon_{n\mathbf{k}} - \zeta)^2}{T}\frac{\partial f^0(\varepsilon_{n\mathbf{k}}, \zeta, T)}{\partial \varepsilon_{n\mathbf{k}}}, \quad (3)$$

the electronic thermal conductivity can be further simplified to be

$$\kappa_{el}^{\alpha\beta} = \frac{1}{N_{\mathbf{k}}}\sum_{n\mathbf{k}} c_{el,n\mathbf{k}} v_{n\mathbf{k}}^{\alpha} v_{n\mathbf{k}}^{\beta} \tau_{n\mathbf{k}}^{\kappa}(\varepsilon_{n\mathbf{k}}, \zeta, T), \quad (4)$$

where $c_{el,n\mathbf{k}}$ is the mode resolved electron specific heat. The specific heat and group velocity can be determined from the electronic structure, while the calculation of relaxation time is more complicated. At intermediate temperature range, the dominant scattering mechanism for electron is electron-phonon scattering [42]. The expression and calculation method of electron transport relaxation time considering this scattering mechanism can be obtained in our previous work [42]. Note that one can also calculate the transport properties from the iterative method, which is believed to be more accurate [43,44]. In this work we still adopted relaxation time approximation (RTA) based on the following considerations. First, for metals, the electron-phonon scatterings around 300 K and above are isotropic and elastic [14,45], and therefore the difference between the iterative method and RTA is expected to be small. Second, RTA requires a relatively small computational cost. Third, RTA can give exact relaxation time values, which allows us to better analyze the results.

The phonon thermal conductivity can be expressed with [46,47]

$$\kappa_{\mathrm{ph}}^{\alpha\beta} = \frac{1}{N_{\mathbf{q}}}\sum_{\lambda} c_{\mathrm{ph},\lambda} v_{\lambda}^{\alpha} v_{\lambda}^{\beta} \tau_{\lambda}, \quad (5)$$

where $N_{\mathbf{q}}$ is the total number of $\mathbf{q}$ points sampled in the Brillouin zone, $c_{\mathrm{ph},\lambda}$ [48] is the mode resolved phonon heat capacity for phonon mode λ, v_{λ}^{α} and v_{λ}^{β} are the phonon group velocity at the α and β directions, and τ_{λ} is the phonon relaxation time, which mainly considers phonon-phonon scattering and phonon-electron scattering at the temperature range we consider. The specific heat $c_{\mathrm{ph},\lambda}$ and group velocity

v_λ can be calculated from the phonon dispersion relations. The relaxation time considering both phonon-phonon scattering and phonon-electron scattering can be determined by the Matthiessen rule [49] as $1/\tau_\lambda = 1/\tau_{\lambda,pp} + 1/\tau_{\lambda,pe}$, where $1/\tau_{\lambda,pp}$ is the phonon-phonon scattering rate and $1/\tau_{\lambda,pe}$ is the phonon-electron scattering rate. The details for calculating $1/\tau_{\lambda,pe}$ and $1/\tau_{\lambda,pp}$ can be found in Ref. [39].

The first-principles calculations are carried out with QUANTUM ESPRESSO [50]. To obtain lattice constants that can better match the experimental data, we employ norm-conserving pseudopotentials [51] with the Perdew-Burke-Ernzerhof form of the exchange-correlation functional [52] for Pt and Al, while the Perdew-Zunger parametrization [53] and Bachelet-Hamann-Schlüter type norm-conserving pseudopotentials [54] with local density approximation for the exchange-correlation functional are employed for W. The comparison between the pressure-volume relations is shown in Fig. 2. We also consider the spin-orbit coupling (SOC) effect for Pt because of the more accurate band structure around the Fermi energy for calculation with SOC [40]. The cutoff energy of the plane wave is set as 120 Ry, while the convergence threshold of electron energy is set to be 10^{-10} Ry for the self-consistent field calculation. The phonon dispersion relations are calculated by density functional perturbation theory [55], with a $6 \times 6 \times 6$ **q** grid and a self-consistency threshold of 10^{-15} Ry. The phonon-phonon scattering rate is calculated with the density functional perturbation method using the D3Q package [56]. Since the SOC has little effect on the force constants and phonon frequencies, with details in Appendix C, it is not considered in phonon thermal conductivity calculations. The electron-phonon scattering rate and phonon-electron scattering rate are computed using the electron-phonon Wannier (EPW) code [57]. Using the maximally localized Wannier functions basis [58], the electron-phonon matrix elements, band energies, and phonon modes are interpolated from an initial coarse grid of $12 \times 12 \times 12$ and $6 \times 6 \times 6$ electron and phonon vector grids, respectively, to dense grids of $60 \times 60 \times 60$ and $40 \times 40 \times 40$ electron and phonon vector grids, respectively.

In the subsequent discussions we also compare our predictions with the widely used theoretical model developed by Bohlin [26]. The theoretical model for pressure-dependent electronic thermal conductivity is included in Appendix A.

III. RESULTS AND DISCUSSIONS

A. Validations at 0 GPa

In order to validate our first-principles simulations, we first study the lattice constants, as well as the temperature-dependent electrical conductivity and thermal conductivity at 0 GPa. The lattice constants are determined to be 4.02 Å for Al, 3.93 Å for Pt, and 3.12 Å for W, while the corresponding experiment values are 4.04 Å [59], 3.92 Å, and 3.16 Å [60], respectively. All three lattice constants show good agreement with experiment data.

The temperature-dependent electrical conductivity and thermal conductivity of Al, Pt, and W are predicted at 0 GPa, as shown in Fig. 1. Note that phonon thermal conductivity is included in the predicted thermal conductivity. In the range of 200–900 K, electrical conductivity for Al, W, and Pt decreases with temperature. This is related to the increase in electron-phonon scattering rate with increasing temperature [39]. In comparison, the temperature-dependent thermal conductivity shows different trends for different metals. The thermal conductivity of Al becomes nearly temperature independent above 300 K, while the thermal conductivity of Pt increases monotonically when temperature increases. Such trend is related to the competition between the decrease in electron lifetime and the increase in electron specific heat at high temperature, as discussed in Ref. [42]. The temperature dependence of Pt agrees well with previous works [63,67,68]. On the other hand, the thermal conductivity of W decreases with temperature, mainly due to the decrease of phonon thermal conductivity with temperature [41]. Note that we predict that phonon transport contributes 30% to the total thermal conductivity at 300 K for W, similar to previous works.

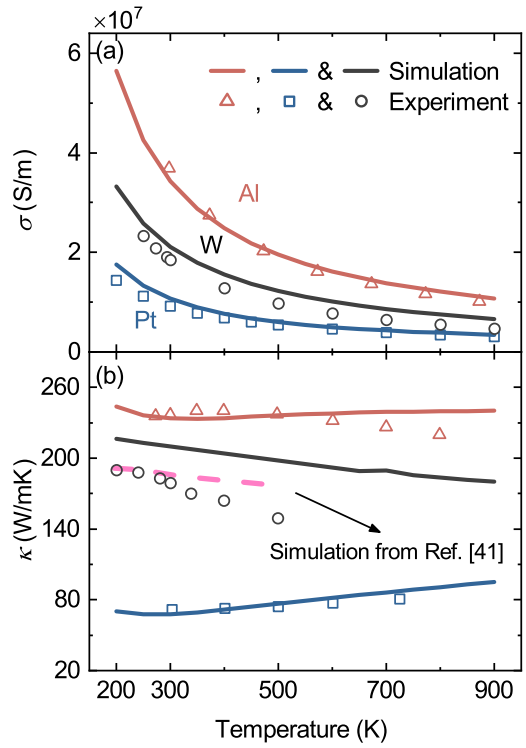

FIG. 1. The temperature-dependent (a) electrical conductivity (σ) and (b) thermal conductivity (κ) of Al, Pt, and W at 0 GPa. The experiment data are taken from Refs. [61–66], while the dashed line in (b) shows the simulation results from the literature [41].

Compared to the experiment data, the predicted electrical conductivity and thermal conductivity all show quantitative agreement with experimental results. This confirms that our mode-level first-principles calculation is reliable and can be further adopted to the study of the pressure effect. There is a slight deviation in the thermal conductivity of W from the experimental results [66], which may be related to the slightly smaller lattice constant predicted by first-principles calculations [69]. Above 300 K, the deviation between experimental results and simulation results becomes larger, which is also seen in the previous work [41].

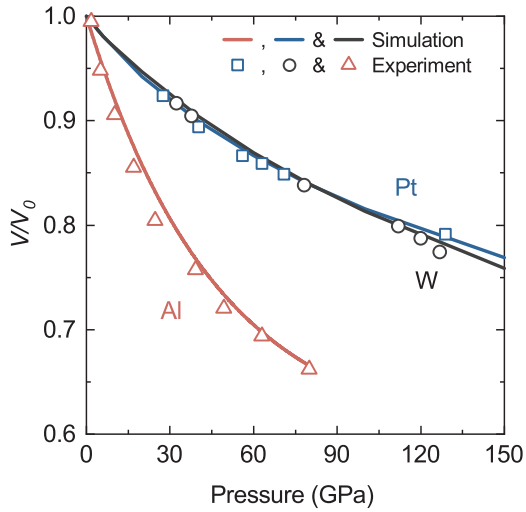

FIG. 2. Normalized unit cell volume V as a function of pressure from first-principles calculation and the comparison with experiment data of Al [70], Pt [71], and W [72]. The volume is normalized by unit cell volume V_0 at 0 GPa.

B. Pressure-dependent electronic thermal conductivity

Before studying the pressure dependence of thermal conductivity, we first study the pressure dependence of normalized unit cell volume V/V_0, as shown in Fig. 2. The normalized volumes of Al, W, and Pt are found to decrease with pressure and become less pressure dependent at high pressure. The nonlinear pressure dependence arises from the atomic bond hardening at high pressure. Under the same pressure, Al has the largest volume decrease among these three metals. For instance, Al has around a 20% volume decrease at 30 GPa, while the volume decrease of both W and Pt is less than 10%. The experiment data are also shown in Fig. 2, and are in good agreement with our simulation results.

Since the electron transport properties are closely related to the electron density of states (DOS), we further check the pressure dependence of DOS for these three metals. Electron DOS for Al, W, and Pt at 0 and 80 GPa are presented in Fig. 3. The electron DOS of Al shows free-electron-like parabolas at both 0 and 80 GPa, while the electron DOS of Pt and W have irregular shapes around the Fermi energy. Moreover, the electron DOS of all three metals expand to a larger energy spectrum with pressure. Meanwhile, the peaks of DOS decrease with pressure in all three metals, and likewise, the DOS around the Fermi energy of Al and Pt decrease from 0.40 to 0.24 states/eV atom, and 1.62 to 1.23 states/eV atom, respectively. The electron DOS of W at Fermi energy is nearly pressure independent, which is around 0.41 states/eV atom at both 0 and 80 GPa. Moreover, the contribution from different electron states is also shown in Fig. 3. The electron DOS of Al around Fermi energy is mainly composed of free-electron-like states, the s and p states. Meanwhile, the dominant states of Pt and W are d states. The energy span of d states is narrower than that of free-electron-like s and p states, and therefore less dispersive, which is consistent with a previous study [73]. As will be shown later, different pressure dependence of electronic thermal conductivity is related to the different pressure dependences of electron DOS for Al, Pt, and W.

The pressure dependence of electronic thermal conductivity is shown in Fig. 4(a). We consider the temperature of 300 K for the subsequent discussions on the pressure effect of

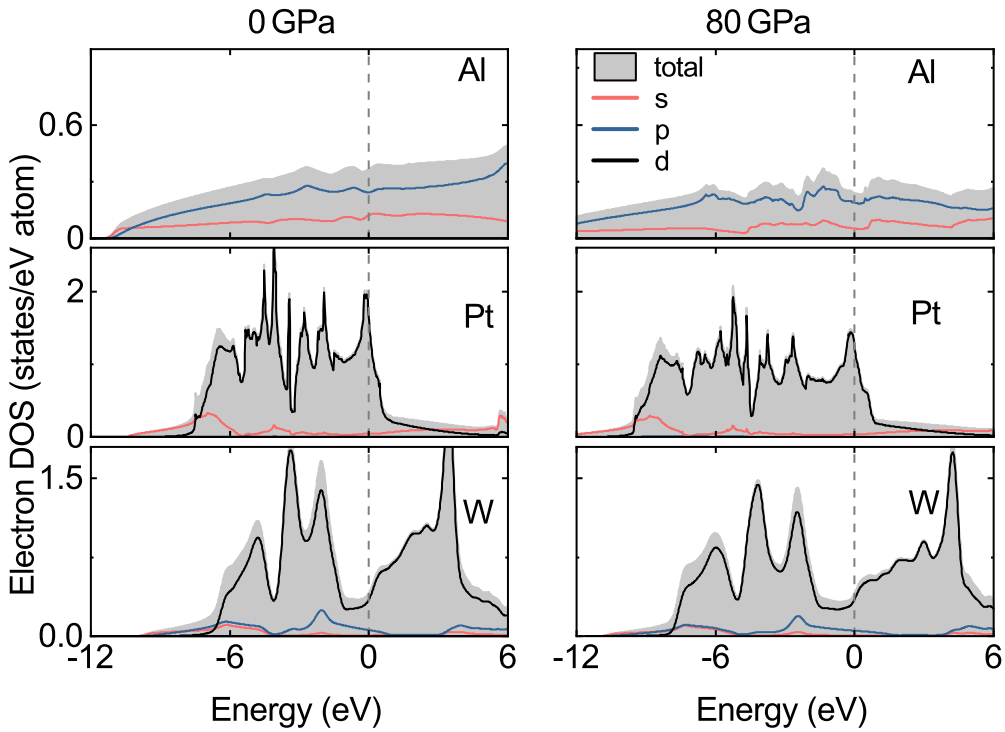

FIG. 3. Electron density of states of Al, Pt, and W at 0 and 80 GPa.

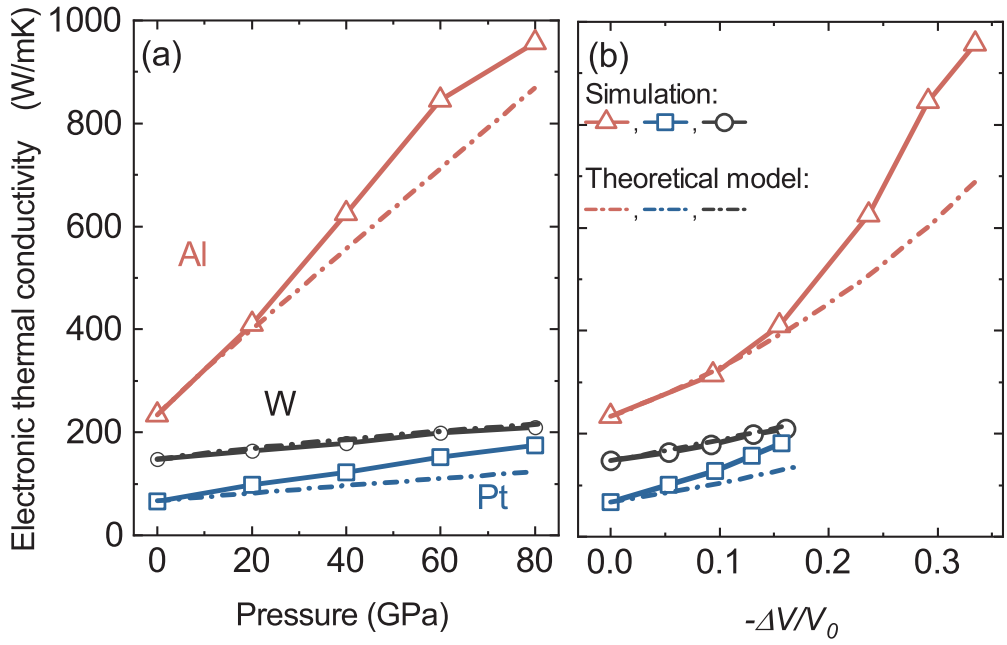

FIG. 4. Thermal conductivity of Al, Pt, and W at 300 K as a function of pressure (a) and (b) normalized volume reduction. Our simulation results are compared with the theoretical model which is shown by dot-dash lines.

thermal conductivity. When pressure increases, the electronic thermal conductivity of Al, W, and Pt increases almost linearly with pressure. The electronic thermal conductivity of Al, Pt, and W is 234, 64, and 147 W/mK, respectively, at 0 GPa, while their electronic thermal conductivity increases to 957, 175, and 210 W/mK, respectively, at 80 GPa. The electronic thermal conductivity of Al has the largest pressure dependence among these three metals. This is related to the large volume decrease of Al under the same pressure, as illustrated in Fig. 2. Since the pressure effect on solids is essentially through the change of volume, the electronic thermal conductivity as function of volume reduction is shown in Fig. 4(b). When the volume is reduced by around 15%, the electronic thermal conductivity of Al, Pt, and W increases to around 2.0, 2.7, and 1.4 times that at 0 GPa, respectively. Different from the pressure dependence, the thermal conductivity change for Pt is the largest with respect to volume reduction. On the other hand, the volume dependence of the electronic thermal conductivity is not linear, as clearly shown by Al. Also, we can calculate the Lorenz ratio of these three metals under different pressures. The pressure-dependent Lorenz ratio is shown in Appendix B.

For comparison, electronic conductivity predicted by the widely used theoretical model from Ref. [26] (see Appendix A) is also shown in Fig. 4 (results of theoretical model and our simulation for W are almost overlapped). According to Eq. (A3), the variation of thermal conductivity with volume is determined by the Grüneisen parameter and the temperature-dependent parameter ξ. At 300 K, the ξ of Al, W, and Pt are close to each other, and therefore, the different Grüneisen parameters of these three metals lead to different pressure dependences. At 0 GPa, the Grüneisen parameters of Pt, Al, and W are 2.8, 2.0, and 1.8. Therefore, the electronic thermal conductivity of Pt predicted from the theoretical model also has the largest volume dependence, which is consistent with our simulation results. Moreover, results of the theoretical model also have good agreement with the simulation results for Al in the volume reduction range of 0%–15%. However, with even larger volume reduction, the theoretical model underestimates the electronic thermal conductivity of Al. As for Pt, the theoretical model underestimates the increase of thermal conductivity even for small volume reduction. As for W, the theoretical model seems to give quite good predictions of the electronic thermal conductivity.

In order to understand the different pressure effects on electronic thermal conductivity, we further analyze the pressure dependence of the three electron properties based on Eq. (4), which are the electron specific heat (C_{el}), the square of group velocity (v^2), and the lifetime due to electron-phonon scattering (τ^κ). The pressure effect on these properties of Al, W, and Pt is normalized and illustrated in Fig. 5. Note that the group velocity and relaxation time are different for different modes, and therefore the average values are presented, which are defined as

$$\langle \tau^\kappa \rangle = \frac{\sum_{n\mathbf{k}} |v_{n\mathbf{k}}|^2 \tau^\kappa_{n\mathbf{k}} \frac{\partial f^0}{\partial \varepsilon_{n\mathbf{k}}}}{\sum_{n\mathbf{k}} |v_{n\mathbf{k}}|^2 \frac{\partial f^0}{\partial \varepsilon_{n\mathbf{k}}}}, \tag{6}$$

$$\langle v^2 \rangle = \frac{\sum_{n\mathbf{k}} |v_{n\mathbf{k}}|^2 \frac{\partial f^0}{\partial \varepsilon_{n\mathbf{k}}}}{\sum_{n\mathbf{k}} \frac{\partial f^0}{\partial \varepsilon_{n\mathbf{k}}}}. \tag{7}$$

For Al, both C_{el} and $\langle v^2 \rangle$ have small variation with pressure. The small variation in C_{el} can be attributed to the trade-off between the decreasing electron DOS (Fig. 3) and the simultaneously decreased volume. In comparison, the electron lifetime of Al largely increases with pressure and

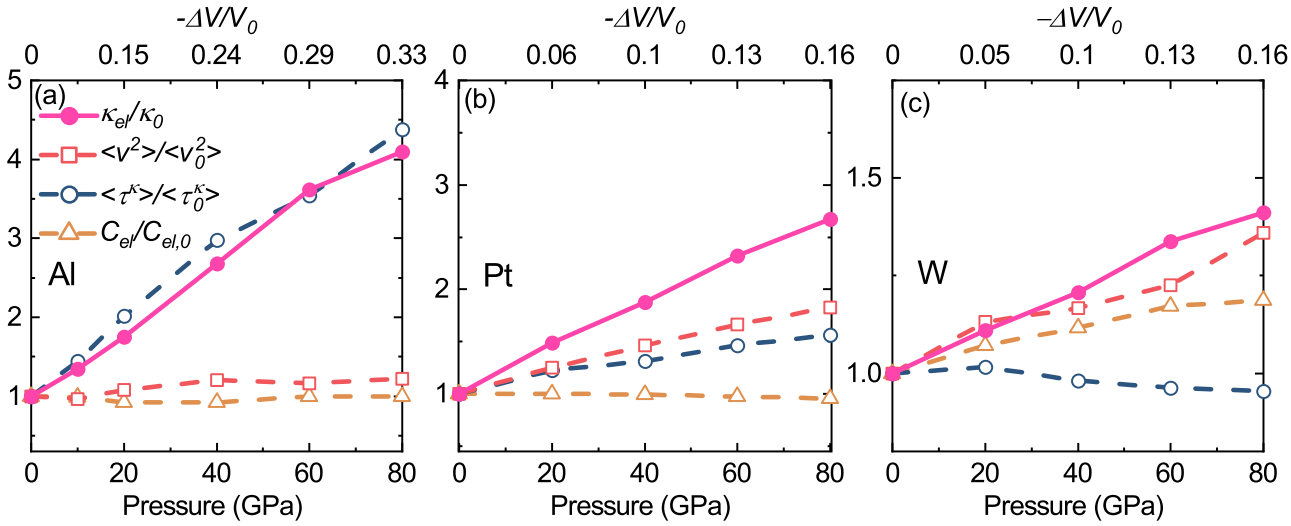

FIG. 5. Normalized electronic thermal conductivity ($\kappa_{el}/\kappa_{el,\,0}$), averaged square velocity ($\langle v^2\rangle/\langle v_0^2\rangle$), relaxation time ($\langle\tau^\kappa\rangle/\langle\tau_0^\kappa\rangle$), and total electron specific heat ($C_{el}/C_{el,0}$) of (a) Al, (b) Pt, and (c) W as a function of pressure.

has a similar trend as the pressure-dependent electronic thermal conductivity. Therefore, the dominant contribution for the increase of electronic thermal conductivity under pressure is the increase of τ^κ, which is consistent with previous works [15].

On the other hand, the mechanism of pressure dependence on Pt is shown to be different from that of Al. As illustrated in Fig. 5(b), the electron specific heat of Pt also has small variation with pressure. However, both group velocity and electron lifetime significantly increase under pressure. At 80 GPa, the averaged square of electron velocity is around 1.8 times that of the 0 GPa value, while the electron lifetime is 1.6 times that of the 0 GPa value. The increase of the squared group velocity even surpasses the increase of electron lifetime and becomes the main contribution to the increase of electronic thermal conductivity with pressure. The theoretical model fails to predict the large velocity increase under pressure. Therefore, it underestimates the pressure-dependent electronic thermal conductivity of Pt. According to Eq. (A3), the pressure dependence of the electronic thermal conductivity of metals are determined by the summation of two terms. The first term, $\xi\gamma$, represents the pressure dependence related to electron-phonon coupling, while the second is a constant term, 1/3. The 1/3 term contains the pressure dependence of the electron group velocity. Notably, the electron-phonon coupling term $\xi\gamma$ is usually much larger than 1/3 [29], and therefore the influence of electron group velocity is small according to the theoretical model. Such small contribution is true for free-electron metals, as illustrated by Al. However, it is not true for complex transition metals such as Pt. It is presumably due to the dominant d states around the Fermi energy of Pt, as shown in Fig. 3. The group velocity of d states has a larger response to the pressure increase than that of free-electron-like s and p states. The electron group velocity is the differential of the electron band energy [49], which is denoted as $v = 1/\hbar(\partial\varepsilon/\partial\boldsymbol{k})$. Therefore, the electron group velocity is closely related to the electron band structure. The energy bands of the d state electrons are limited to a small energy range with respect to the wave vector (less dispersive), while those of free-electron-like electron states have a larger energy range (more dispersive) [74]. Therefore, the electron group velocity of d state electrons is smaller than that of free-electron-like states [74]. The interatomic distance decreases with the increase of pressure. This decrease induces a less effective centrifugal barrier for the d band [75], resulting in an additional energy expansion. As a result, the electron group velocity of d band electrons increases under pressure.

Similar to Pt, the squared velocity of W also makes a dominant contribution to the increase of electronic thermal conductivity with pressure, as illustrated in Fig. 5(c). The d-state electrons are also dominant around the Fermi energy of W. However, the pressure dependence of the specific heat and electron relaxation time of W is different from those of Pt and Al. The electron specific heat shows a positive relationship with pressure. As illustrated in Fig. 3, the electron DOS per atom of W are nearly pressure independent. The decrease of the volume at high pressure consequently leads to an increase in the electron specific heat. On the other hand, the electron lifetime is found to have small variation and has a small decrease under high pressure in W. Such pressure dependence is opposite to the predictions from the theoretical model. The competing effect of these three properties leads to a coincident consistency between the results of the theoretical model and our simulations.

The electron lifetime of both Al and Pt increases with pressure, while the electron lifetime of W decreases with pressure. Therefore, the mechanisms behind it are expected to be different. In order to understand the different mechanisms, we first introduce an intermediate parameter, electron-phonon coupling constant (λ) [32], which is defined as

$$\lambda = 2\int_0^\infty \frac{\alpha^2F(\omega)d\omega}{\omega}, \tag{8}$$

where ω is the phonon frequency, $\alpha^2(\omega)$ is effective electron-phonon coupling function, and $F(\omega)$ is the phonon DOS. The product of $\alpha^2(\omega)$ and $F(\omega)$ is the spectral function $\alpha^2F(\omega)$.

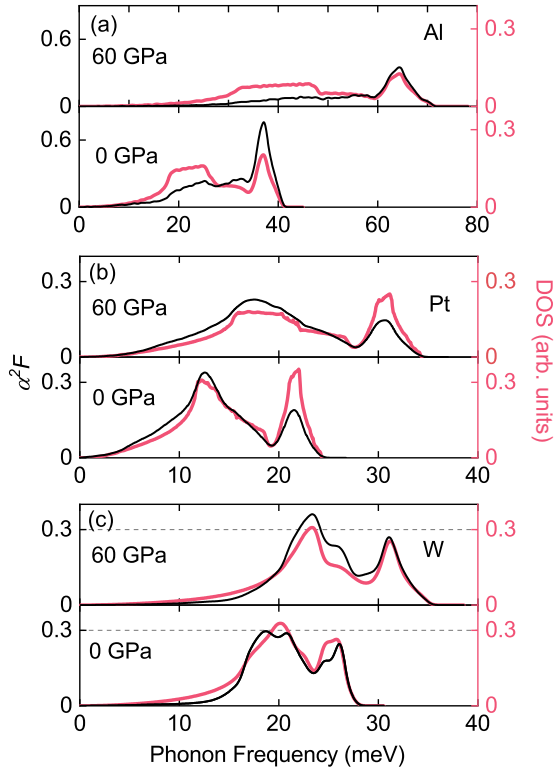

FIG. 6. Variations of $\alpha^2F(\omega)$ and phonon density of states of (a) Al, (b) Pt, and (c) W as a function of phonon frequency.

The λ characterizes the strength of electron-phonon coupling. At high temperatures, the electron relaxation time due to electron-phonon coupling (τ_{ep}) can be approximated by $1/\tau_{ep} = (2\pi/\hbar)\, k_B\, T\lambda$ [32]. From 0 to 60 GPa, the λ of Al, Pt, and W changes from 0.48, 0.51, and 0.26 to 0.17, 0.38, and 0.28, respectively.

The $\alpha^2F(\omega)$ and phonon DOS at 0 and 60 GPa of these three metals are presented in Fig. 6. It is shown that the shape of the $\alpha^2F(\omega)$ is similar to the shape of phonon DOS. At high pressure, the phonon DOS spread to higher frequency, while the phonon DOS at the original frequency range decrease. The large variation of the phonon DOS in Al and Pt under pressure directly influences the pressure dependence of $\alpha^2F(\omega)$. The $\alpha^2F(\omega)$ of these two metals also shifts to higher frequency and its value at original frequency decreases accordingly. According to Eq. (8), the spectral function at higher frequency will have smaller weight in the integral of the electron-phonon coupling constant. Therefore, the overall electron-phonon coupling constant decreases with pressure for Al and Pt. On the other hand, an opposite relation is found in W. The peaks of phonon DOS of W decrease with pressure, while the peaks of the α^2F function increase with pressure. This implies a large increase of the $\alpha^2(\omega)$ function with pressure, which even surpasses the influence from the phonon DOS and leads to an increase of α^2F with pressure. Consequently, the electron-phonon coupling strength increases with pressure in W. The $\alpha^2(\omega)$ characterizes the averaged electron-phonon coupling matrix elements on the Fermi surface, and electron DOS around Fermi energy directly influences the change of $\alpha^2(\omega)$ [32].

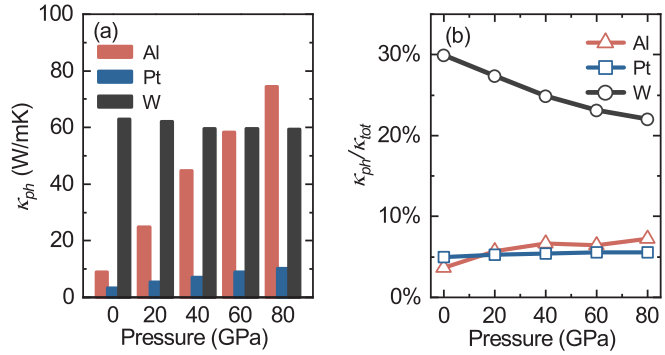

FIG. 7. (a) Phonon thermal conductivity and (b) its ratio in total thermal conductivity of Al, Pt, and W under different pressures.

Therefore, the increase of $\alpha^2(\omega)$ is possibly related to the abnormal electron DOS change of W around the Fermi energy.

C. Pressure-dependent phonon thermal conductivity

We further consider the phonon thermal conductivity under pressure, the results are shown in Fig. 7(a). For both Al and Pt, the phonon thermal conductivity increases with pressure, while the pressure effect is more prominent in Al. From 0 to 80 GPa, the phonon thermal conductivity of Al increases from 9 to 74.6 W/mK, about eight times, while the phonon thermal conductivity of Pt increases from 3.4 to 11.4 W/mK, only around four times. On the other hand, even though the phonon thermal conductivity of W is the largest among these three metals at 0 GPa, it is nearly pressure independent in the pressure range of 0–80 GPa. Because of the different pressure dependence of the electronic and phonon thermal conductivity among these metals, the ratios of phonon thermal conductivity in the total thermal conductivity are expected to be different; these are presented in Fig. 7(b). The ratio of phonon thermal conductivity in Al is 3.7% at 0 GPa, which is the lowest among these three metals. Nonetheless, its ratio increases to 7.2% as the pressure increases to 80 GPa. The ratio of phonon thermal conductivity in Pt is almost pressure independent, due to the comparable pressure dependence of electronic and phonon thermal conductivity. Although the phonon thermal conductivity of W has the highest ratio at 0 GPa, a decrease of the ratio at high pressure is found due to the pressure-independent phonon thermal conductivity and the increase of pressure-dependent electronic thermal conductivity. The ratio of phonon thermal conductivity of W decreases from 30% at 0 GPa to around 20% at 80 GPa. Despite such decrease, the phonon thermal conductivity of W is still non-negligible with pressure up to 80 GPa.

In order to understand different pressure dependence of phonon thermal conductivity for these three metals, an analysis of the phonon mode properties, similar to the electron counterpart, is performed and presented in Fig. 8. The phonon group velocity and relaxation time are average values which are weighted by phonon specific heat, as illustrated in Ref. [76]. Under the same pressure, Al has the largest volume

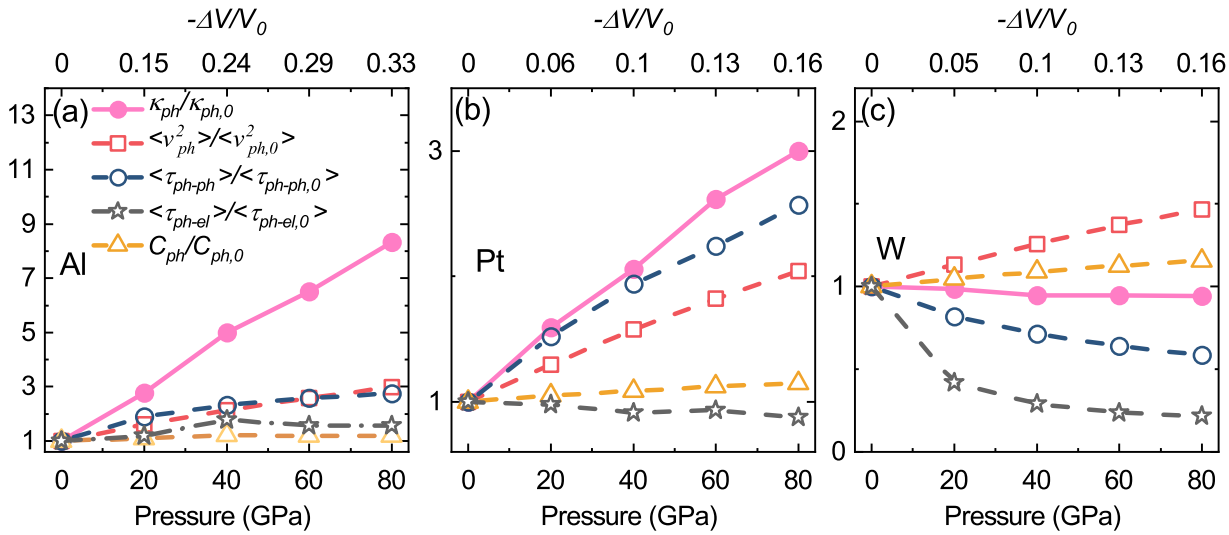

FIG. 8. Normalized phonon thermal conductivity ($\kappa_{\rm ph}/\kappa_{\rm ph,0}$), averaged square of phonon velocity ($\langle v^2_{\rm ph}\rangle/\langle v^2_{\rm ph,0}\rangle$), relaxation time due to phonon-electron scattering ($\langle\tau_{{\rm ph}-el}\rangle/\langle\tau_{{\rm ph}-el,0}\rangle$) and phonon-phonon scattering ($\langle\tau_{{\rm ph}-ph}\rangle/\langle\tau_{{\rm ph}-ph,0}\rangle$) and phonon specific heat ($C_{\rm ph}/C_{\rm ph,0}$) of (a) Al, (b) Pt, and (c) W as a function of pressure.

reduction, and therefore, phonon thermal conductivity of Al has the largest increase. At 15% volume reduction, the phonon thermal conductivity of both Al and Pt increases to around three times the 0 GPa value, while that of W still has small variation. The phonon group velocity of all three metals has a large increase with pressure. For Al and Pt with face centered cubic (fcc) structure, the phonon lifetime due to the phonon-phonon scattering increases in Pt and Al, which is consistent with the pressure dependence in fcc argon crystal [12]. However, the phonon-phonon scattering increases with pressure in W, which is opposite to that in Pt and Al. W has body centered cubic (bcc) structure and has a small phonon-phonon scattering rate at 0 GPa which has been discussed in Ref. [41]. In brief, the small phonon-phonon scattering rate results from the relatively isotropic phonon branches, which have a small difference. Such phonon dispersions provide few scattering channels, so the scattering rate is small. However, under high pressure, the lower transverse acoustic phonon branches along the $\Gamma - N$ direction become relatively softer than other branches [77], and the three phonon branches are relatively far from each other. This change opens more scattering channels and the phonon-phonon scattering is consequently increased under pressure.

One major difference between the phonon thermal conductivity in metals and nonmetals is that an additional scattering mechanism, phonon-electron scattering, influences the phonon transport in metals. As illustrated in Fig. 8, the relaxation time due to the phonon-electron scattering has a small increase with pressure in Al, while that in Pt has a small decrease with pressure. Meanwhile, the phonon-electron scattering increases largely under high pressure in W. The increase in W is likely due to the increase of electron-phonon coupling matrix elements, as indicated by the increase of $\alpha^2(\omega)$ with pressure in W. The increase of phonon group velocity with pressure and the decrease of phonon lifetime are competing mechanisms, and therefore, lead to a pressure invariant phonon thermal conductivity of W.

IV. CONCLUSIONS

In summary, the pressure effect on the electronic and phonon thermal transport properties of W, Pt, and Al is investigated by mode-level first-principles calculations. For electronic thermal conductivity, applying pressure leads to an increase of thermal conductivity for the three metals. However, different mechanisms are found in these metals. For Al, the decrease of the electron-phonon scattering makes a dominant contribution to the increase of electronic thermal conductivity. For Pt and W, the increase of the electron group velocity surpasses the decreasing electron-phonon scattering and becomes the main contribution, mainly due to their dominance of d state electrons around the Fermi energy. Applying pressure also shows a positive effect on the phonon thermal conductivity of Al and Pt, while the phonon thermal conductivity of W is nearly pressure independent. According to the mode property analysis, the phonon group velocity and specific heat of all three metals increases with pressure. The positive pressure dependence of the phonon lifetime is found in both Al and Pt, which eventually results in an increase of their phonon thermal conductivity with pressure. As for W, the phonon lifetime due to both phonon-phonon and phonon-electron scattering decreases with pressure. The collective effects between phonon lifetime and group velocity lead to a pressure invariant phonon thermal conductivity of W.

ACKNOWLEDGMENTS

This work is supported by National Natural Science Foundation of China (Grant No. 52122606). Simulations were performed on the π2.0 cluster supported by the Center for High Performance Computing from Shanghai Jiao Tong University. S.L. acknowledges the support by Shanghai Municipal Natural Science Foundation (Grant No. 22YF1400100) and the Fundamental Research Funds for the Central Universities (Grant No. 2232022D-22).

APPENDIX A: THEORETICAL MODEL OF ELECTRONIC THERMAL CONDUCTIVITY

The theoretical model for pressure-dependent electronic thermal conductivity also starts from the BTEs. In order to obtain a compact and treatable solution, this model implements the Debye model for phonons and the free-electron model for electrons [78]. An expression for electronic thermal conductivity is given by [26]

$$\frac{1}{\kappa_{el}} = 4\frac{Cq_F}{\theta_D}\frac{1}{L_0 T}\left\{\left(\frac{T}{\theta_D}\right)^5 J_5\left(\frac{\theta_D}{T}\right)\left[1+\frac{3}{\pi^2}\left(\frac{k_F}{q_D}\right)\left(\frac{\theta_D}{T}\right)^2 - \frac{1}{2\pi^2}\frac{J_7\left(\frac{\theta_D}{T}\right)}{J_5\left(\frac{\theta_D}{T}\right)}\right]\right\}, \tag{A1}$$

where C is a constant independent of the volume; θ_D is the Debye temperature; L_0 is the Sommerfeld value; T is the temperature; k_F and q_D are the Fermi and Debye wave numbers, respectively [74]. $J_n(x)$ is the Debye integral defined as

$$J_n(x) = \int_0^x \frac{z^n e^z}{(e^z-1)^2} dz. \tag{A2}$$

Reviewing the above equation, it implies that only k_F contains the information of the electron information, while all the information of electron phonon coupling is related to the Debye temperature θ_D. The change of $1/\kappa_{el}$ with respect to volume can be obtained by [26]

$$\frac{\partial \ln(1/\kappa_{el})}{\partial \ln V} = \gamma - \frac{1}{3} - \gamma\frac{\partial\left\{x^{-5}J_5(x)\left[1+\frac{3}{\pi^2}(k_F/q_D)x^2 - \frac{1}{2\pi^2}J_7(x)/J_5(x)\right]\right\}}{\partial \ln x}, \tag{A3}$$

where x is defined as $x = \theta_D/T$; γ is the Grüneisen parameter which is defined as $\gamma = -\ln\theta_D/\ln V$. Since k_F/q_D is a constant according to Ref. [74], the differentiation with respect to x is a universal coefficient independent of materials but dependent on temperature. Temperature dependence of this term can be found in Ref. [26]. Therefore, we can simplify the right side of Eq. (A3) as $\xi\gamma - 1/3$, where ξ is the universal coefficient which equals the summation of the coefficient before γ. The Grüneisen parameter can be calculated from the mode Grüneisen parameter γ_λ, whose relation is [79]

$$\gamma = \frac{\sum_\lambda \gamma_\lambda c_{\mathrm{ph},\lambda}}{\sum_\lambda c_{\mathrm{ph},\lambda}}. \tag{A4}$$

For the theoretical model, the mode Grüneisen parameters at discrete volumes are obtained by PHONOPY [80]. Since the calculation of the electronic thermal conductivity requires an integral involving Grüneisen parameters, an expression of Grüneisen parameters versus volumes is fitted by those discrete values using the expression given in Ref. [81]. Debye temperature θ_D is related to the Grüneisen parameters $\gamma = -(\partial\ln\theta_D/\partial\ln V)$. Therefore, the Debye temperature can be further determined by integrating the Grüneisen parameters with respect to volume,

$$\theta_D(V) = \theta_0\left(\frac{V}{V_0}\right)^{-\gamma_\infty}\exp\left(-\left\{3a\left[\left(\frac{V}{V_0}\right)^{1/3}-1\right] + \frac{b}{n}\left[\left(\frac{V}{V_0}\right)^n - 1\right]\right\}\right), \tag{A5}$$

where γ_∞ is the value of the Grüneisen parameter when the pressure approaches infinity, which is 1/2 or 2/3 based on the Thomas-Fermi theory [81]; V is the volume of materials, and normalized by 0 GPa value V_0; a, b, and n are the parameters which need to be determined by fitting the Grüneisen parameters calculated from first-principles calculation under different pressure; θ_0 is the Debye temperature at 0 GPa.

APPENDIX B: LORENZ RATIO AT DIFFERENT PRESSURES

In experiments, the Wiedemann-Franz law is usually employed to evaluate the thermal conductivity of metals, as $\kappa = L\sigma T$, with L the Lorenz ratio. The Sommerfeld value ($L_0 = 2.44\times10^{-8}\ \mathrm{W\,\Omega/K^2}$) is widely used in practice. This postulate is valid based on two conditions: (1) the phonon thermal conductivity can be ignored; (2) the electron-phonon scattering is elastic. The Lorenz ratios corresponding to electron thermal conductivity (L_e) and total thermal conductivity

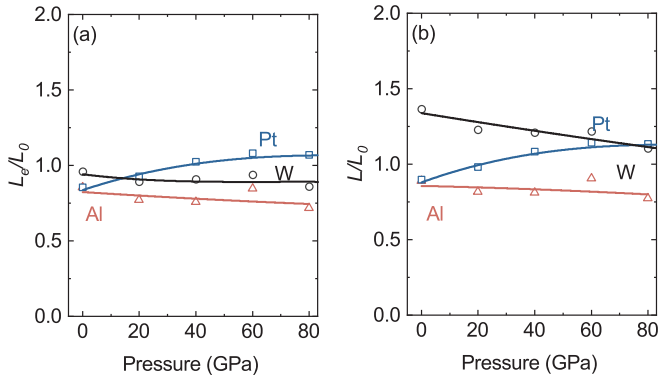

FIG. 9. Lorenz ratio of Al, Pt, and W under different pressure.

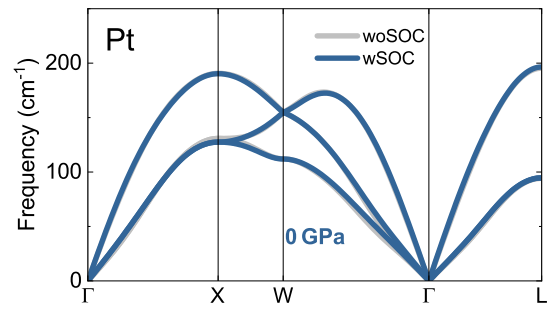

FIG. 10. Comparison between the phonon dispersion relations of Pt with SOC and without SOC.

(L) of these three metals are shown in Fig. 9. The L_e of Al and W has little departure from the Sommerfeld value under different pressure. Meanwhile, L_e of Pt has a slight increase with pressure.

The L and L_e of Al and Pt are close to each other. This is attributed to the relatively small phonon thermal conductivity. On the other hand, L of W is around 30% larger than L_0 at 0 GPa due to the large contribution from phonon thermal conductivity, which is also observed in Ref. [41]. However, L of W decreases to L_0 as pressure increases. It is related to the decrease in the ratio of phonon thermal conductivity under high pressure, as shown in Fig. 7(b).

APPENDIX C: EFFECT OF SPIN-ORBITAL COUPLING ON PHONON TRANSPORT

Spin-orbital coupling (SOC) effect is a relativistic effect which is known to cause the electron band splitting and the opening band gap [82] in electron band structure. However, the SOC effect can be neglected in the investigation of phonon transport. As seen from the details in Fig. 10, the phonon dispersions of Pt with/without SOC are almost identical. Therefore, the SOC has little effect on force constants and thermal conductivity. We believe it is reasonable to turn off the SOC in phonon thermal conductivity calculation considering only phonon-phonon scattering.

Furthermore, we employ the SHENGBTE package [47] which can consider the SOC to calculate the phonon thermal conductivity to verify the above postulation. The resulting phonon thermal conductivity at 300 K and 0 GPa is 7.71 and 8.25 W/mK without the SOC and with the SOC, respectively. The small difference suggests that the phonon thermal conductivity obtained from D3Q without considering the SOC effect is reliable.

[1] M. Pozzo, C. Davies, D. Gubbins, and D. Alfe, Nature (London) **485**, 355 (2012).
[2] G. T. Hohensee, M. R. Fellinger, D. R. Trinkle, and D. G. Cahill, Phys. Rev. B **91**, 205104 (2015).
[3] Y. Song, K. He, J. Sun, C. Ma, M. Wan, Q. Wang, and Q. Chen, Sci. Rep. **9**, 4172 (2019).
[4] L. Elalfy, D. Music, and M. Hu, Materials **12**, 3491 (2019).
[5] J. Prado-Gonjal, F. Serrano-Sánchez, N. Nemes, O. Dura, J. Martínez, M. Fernández-Díaz, F. Fauth, and J. Alonso, Appl. Phys. Lett. **111**, 083902 (2017).
[6] A. Kosuga, K. Umekage, M. Matsuzawa, Y. Sakamoto, and I. Yamada, Inorg. Chem. **53**, 6844 (2014).
[7] A. Kamegawa, Y. Goto, R. Kataoka, H. Takamura, and M. Okada, Renewable Energy **33**, 221 (2008).
[8] H. Vollstädt, E. Ito, M. Akaishi, S.-i. Akimoto, and O. Fukunaga, Proc. Jpn. Acad., Ser. B **66**, 7 (1990).
[9] Y. Nishihara, K. Fuke, Y. Tange, and Y. Higo, High Press. Res. **36**, 121 (2016).
[10] I. Getting and G. Kennedy, J. Appl. Phys. **41**, 4552 (1970).
[11] D. A. Broido, L. Lindsay, and A. Ward, Phys. Rev. B **86**, 115203 (2012).
[12] K. D. Parrish, A. Jain, J. M. Larkin, W. A. Saidi, and A. J. H. McGaughey, Phys. Rev. B **90**, 235201 (2014).
[13] N. K. Ravichandran and D. Broido, Nat. Commun. **10**, 827 (2019).
[14] Y. Zhou, Z.-Y. Dong, W.-P. Hsieh, A. F. Goncharov, and X.-J. Chen, Nat. Rev. Phys. **4**, 319 (2022).
[15] A. Giri, J. T. Gaskins, L. Li, Y.-S. Wang, O. V. Prezhdo, and P. E. Hopkins, Phys. Rev. B **99**, 165139 (2019).
[16] Y. Zhang, M. Hou, G. Liu, C. Zhang, V. B. Prakapenka, E. Greenberg, Y. Fei, R. E. Cohen, and J.-F. Lin, Phys. Rev. Lett. **125**, 078501 (2020).
[17] L. V. Pourovskii, J. Mravlje, M. Pozzo, and D. Alfe, Nat. Commun. **11**, 4105 (2020).
[18] Z. Tong, S. Li, X. Ruan, and H. Bao, Phys. Rev. B **100**, 144306 (2019).
[19] Y. Wang, Z. Lu, and X. Ruan, J. Appl. Phys. **119**, 225109 (2016).
[20] H.-K. Mao, X.-J. Chen, Y. Ding, B. Li, and L. Wang, Rev. Mod. Phys. **90**, 015007 (2018).
[21] H. Mao, Science **200**, 1145 (1978).
[22] L. Wang, Y. Ding, W. Yang, W. Liu, Z. Cai, J. Kung, J. Shu, R. J. Hemley, W. L. Mao, and H.-k. Mao, Proc. Natl. Acad. Sci. USA **107**, 6140 (2010).
[23] R. S. McWilliams, Z. Konôpková, and A. F. Goncharov, Phys. Earth Planet. Inter. **247**, 17 (2015).
[24] Z. Konopkova, R. S. McWilliams, N. Gomez-Perez, and A. F. Goncharov, Nature (London) **534**, 99 (2016).
[25] K. Ohta, Y. Kuwayama, K. Hirose, K. Shimizu, and Y. Ohishi, Nature (London) **534**, 95 (2016).
[26] L. Bohlin, Solid State Commun. **19**, 389 (1976).
[27] F. Bloch, Z. Phys. **52**, 555 (1929).
[28] E. Grüneisen, Ann. Phys. (Berlin, Ger.) **408**, 530 (1933).
[29] R. G. Ross, P. Andersson, B. Sundqvist, and G. Backstrom, Rep. Prog. Phys. **47**, 1347 (1984).
[30] H. Gomi and T. Yoshino, Phys. Rev. B **100**, 214302 (2019).
[31] J. Xu, P. Zhang, K. Haule, J. Minar, S. Wimmer, H. Ebert, and R. E. Cohen, Phys. Rev. Lett. **121**, 096601 (2018).
[32] P. Allen, Phys. Rev. B **17**, 3725 (1978).
[33] N. A. Lanzillo, J. B. Thomas, B. Watson, M. Washington, and S. K. Nayak, Proc. Natl. Acad. Sci. USA **111**, 8712 (2014).
[34] S. Y. Savrasov and D. Y. Savrasov, Phys. Rev. B **54**, 16487 (1996).
[35] L. Dong, X. Wu, Y. Hu, X. Xu, and H. Bao, Chin. Phys. Lett. **38**, 027202 (2021).
[36] S. Li, X. Zhang, and H. Bao, Phys. Chem. Chem. Phys. **23**, 5956 (2021).
[37] Z. Tong and H. Bao, Int. J. Heat Mass Transfer **117**, 972 (2018).
[38] A. Wang, S. Li, X. Zhang, and H. Bao, Phys. Rev. Mater. **6**, 014009 (2022).
[39] S. Li, A. Wang, Y. Hu, X. Gu, Z. Tong, and H. Bao, Mater. Today Phys. **15**, 100256 (2020).
[40] G. Y. Guo, S. Murakami, T. W. Chen, and N. Nagaosa, Phys. Rev. Lett. **100**, 096401 (2008).
[41] Y. Chen, J. Ma, and W. Li, Phys. Rev. B **99**, 020305 (2019).
[42] S. Li, Z. Tong, X. Zhang, and H. Bao, Phys. Rev. B **102**, 174306 (2020).

[43] W. Li, Phys. Rev. B **92**, 075405 (2015).
[44] J.-J. Zhou, J. Park, I. T. Lu, I. Maliyov, X. Tong, and M. Bernardi, Comput. Phys. Commun. **264**, 107970 (2021).
[45] M. Lundstrom, *Fundamentals of Carrier Transport* (Cambridge University Press, Cambridge, UK, 1990).
[46] D. A. Broido, M. Malorny, G. Birner, N. Mingo, and D. A. Stewart, Appl. Phys. Lett. **91**, 231922 (2007).
[47] W. Li, J. Carrete, N. A. Katcho, and N. Mingo, Comput. Phys. Commun. **185**, 1747 (2014).
[48] J. E. Turney, E. S. Landry, A. J. H. McGaughey, and C. H. Amon, Phys. Rev. B **79**, 064301 (2009).
[49] U. Mizutani, *Introduction to the Electron Theory of Metals* (Cambridge University Press, Cambridge, UK, 2001).
[50] P. Giannozzi, S. Baroni, N. Bonini, M. Calandra, R. Car, C. Cavazzoni, D. Ceresoli, G. L. Chiarotti, M. Cococcioni, and I. Dabo, J. Phys.: Condens. Matter **21**, 395502 (2009).
[51] D. Hamann, Phys. Rev. B **88**, 085117 (2013).
[52] J. P. Perdew, K. Burke, and M. Ernzerhof, Phys. Rev. Lett. **77**, 3865 (1996).
[53] J. P. Perdew and A. Zunger, Phys. Rev. B **23**, 5048 (1981).
[54] G. B. Bachelet, D. R. Hamann, and M. Schlüter, Phys. Rev. B **26**, 4199 (1982).
[55] S. Baroni, S. De Gironcoli, A. Dal Corso, and P. Giannozzi, Rev. Mod. Phys. **73**, 515 (2001).
[56] G. Fugallo, M. Lazzeri, L. Paulatto, and F. Mauri, Phys. Rev. B **88**, 045430 (2013).
[57] S. Poncé, E. R. Margine, C. Verdi, and F. Giustino, Comput. Phys. Commun. **209**, 116 (2016).
[58] A. A. Mostofi, J. R. Yates, G. Pizzi, Y.-S. Lee, I. Souza, D. Vanderbilt, and N. Marzari, Comput. Phys. Commun. **185**, 2309 (2014).
[59] F. Tang, X. Che, W. Lu, G. Chen, Y. Xie, and W. Yu, Phys. B: Condens. Matter **404**, 2489 (2009).
[60] W. D. Callister and D. G. Rethwisch, *Callister's Materials Science and Engineering* (Wiley, Hoboken, NJ, 2020).
[61] L. Binkele and M. Brunen, Thermal conductivity, electrical resistivity and Lorenz function data for metallic elements in the range 273 to 1500 K, Institut für Werkstoffe Energietechnik Report, 1994.
[62] R. Brandt and G. Neuer, Int. J. Thermophys. **28**, 1429 (2007).
[63] R. P. Bhatta, S. Annamalai, R. K. Mohr, M. Brandys, I. L. Pegg, and B. Dutta, Rev. Sci. Instrum. **81**, 114904 (2010).
[64] J. W. Arblaster, Johnson Matthey Technol. Rev. **59**, 174 (2015).
[65] P. Paufler, Cryst. Res. Technol. **18**, 1546 (1983).
[66] H. Landolt and R. Börnstein, *Semiconductors, Physics of IV, III-V, II-VI and I-VII Compounds* (Springer, Berlin, Germany, 1982).
[67] B. Y. Terada, K. Ohkubo, and T. Mohri, Platinum Met. Rev. **49**, 21 (2005).
[68] J. J. Martin, P. H. Sidles, and G. C. Danielson, J. Appl. Phys. **38**, 3075 (1967).
[69] R. Bauer, A. Schmid, P. Pavone, and D. Strauch, Phys. Rev. B **57**, 11276 (1998).
[70] D. Munson and L. Barker, J. Appl. Phys. **37**, 1652 (1966).
[71] M. Matsui, E. Ito, T. Katsura, D. Yamazaki, T. Yoshino, A. Yokoyama, and K.-i. Funakoshi, J. Appl. Phys. **105**, 013505 (2009).
[72] K. V. Khishchenko, J. Phys.: Conf. Ser. **653**, 012081 (2015).
[73] M. Xu, J.-Y. Yang, S. Zhang, and L. Liu, Phys. Rev. B **96**, 115154 (2017).
[74] J. Ziman, *Electrons and Phonons: The Theory of Transport Phenomena in Solids* (Clarendon Press, Oxford, UK, 1960).
[75] N. E. Christensen and B. Seraphin, Phys. Rev. B **4**, 3321 (1971).
[76] K. Ghosh, A. Kusiak, and J.-L. Battaglia, Phys. Rev. B **102**, 094311 (2020).
[77] R. C. Ehemann, J. W. Nicklas, H. Park, and J. W. Wilkins, Phys. Rev. B **95**, 184101 (2017).
[78] T. M. Tritt, *Thermal Conductivity: Theory, Properties, and Applications* (Springer Science & Business Media, New York, 2005).
[79] H.-M. Kagaya and T. Soma, Solid State Commun. **58**, 479 (1986).
[80] A. Togo and I. Tanaka, Scr. Mater. **108**, 1 (2015).
[81] S. K. Sharma, Solid State Commun. **149**, 2207 (2009).
[82] T. Wu, X. Chen, H. Xie, Z. Chen, L. Zhang, Z. Pan, and W. Zhuang, Nano Energy **60**, 673 (2019).